Bioorganic & Medicinal Chemistry Letters 25 (2015) 1864–1868

Contents lists available at ScienceDirect

Bioorganic & Medicinal Chemistry Letters

journal homepage: www.elsevier.com/locate/bmcl

Evolution and synthesis of novel orally bioavailable inhibitors of PDE10A ☆

Douglas F. Burdi *, John E. Campbell †, Jun Wang ‡, Sufang Zhao ‡, Hua Zhong §, Jianfeng Wei §, Una Campbell, Liming Shao ¶, Lee Herman, Patrick Koch, Philip G. Jones, Michael C. Hewitt ||

Sunovion Pharmaceuticals Inc., 84 Waterford Drive, Marlborough, MA 01752, United States

ARTICLE INFO

Article history:
Received 17 November 2014
Revised 17 March 2015
Accepted 18 March 2015
Available online 26 March 2015

Keywords:
PDE10A
PDE10A inhibitor
Phosphodiesterase inhibitor
PCP-induced hyperlocomotion
Schizophrenia

ABSTRACT

The design and synthesis of highly potent, selective orally bioavailable inhibitors of PDE10A is reported. Starting with an active compound of modest potency from a small focused screen, we were able to evolve this series to a lead molecule with high potency and selectivity versus other PDEs using structure-based design. A systematic refinement of ADME properties during lead optimization led to a lead compound with good half-life that was brain penetrant. Compound **39** was highly potent versus PDE10A (IC_{50} = 1.0 nM), demonstrated high selectivity (>1000-fold) against other PDEs and was efficacious when dosed orally in a rat model of psychosis, PCP-induced hyperlocomotion with an EC_{50} of 1 mg/kg.

The cyclic nucleotide phosphodiesterases are a class of enzymes that regulate signal transduction by hydrolyzing the 3′-5′-monophosphate bond of the second messengers 3′,5′-adenosine monophosphate (cAMP) and 3′,5′-guanosine monophosphate (cGMP). There are 11 distinct families of phosphodiesterases, designated PDE1 through PDE11, which vary in their sequence, localization and substrate specificities for cAMP and cGMP.[1] Some PDE family members hydrolyze cAMP or cGMP selectively, while others, so called dual-substrate PDE's, hydrolyze both.[2] PDE10A falls into the latter category, and hydrolyzes cAMP with a higher affinity (K_m = 0.05 μM) than cGMP (K_m = 3 μM).[3]

The high expression level of PDE10A in the striatum has made it a target of great interest in diseases associated with basal ganglia dysfunction, such as schizophrenia and Huntington's Disease.[4] Although PDE10A inhibitors are active in the rodent phencyclidine (PCP) and amphetamine (AMPH)-induced hyperlocomotion models of antipsychotic activity, recent clinical trials in schizophrenia have been a disappointment.[5] With results showing a neuroprotective role for chronic PDE10A inhibition in a mouse model of Huntington's Disease,[6,7] attention lately has turned to this disorder as a potential indication.

Our search for PDE10A inhibitors began with a focused screen[8] of a proprietary set of 5040 compounds, and yielded triazole **1** (Fig. 1) as an initial hit.

Compound **1** displayed modest potency against PDE10A (IC_{50} = 5 μM) and showed little or no inhibition of other phosphodiesterases. However, a broad survey of 87 purchased thioether analogs offered no improvement in potency (data not shown), so our efforts turned to modification of the two-atom linker. To this end, imidazole **2** was synthesized and identified as a promising hit, with an improved IC_{50} of 65 nM, and good selectivity against other phosphodiesterases.

The synthesis of **2** is shown in Scheme 1. Acylation of 5-phenyl-1*H*-imidazole with dimethylsulfamoyl chloride afforded **3**, which was formylated at the 2-position using LDA/DMF to afford **4**. Coupling of **4** to 2-methylquinazolin-4(3*H*)-one was achieved using zinc chloride in acetic acid, and afforded **5**. Reduction of **5** using catalytic hydrogenation afforded **2**.

☆ Atomic coordinates of the PDE10A crystal structure with compound **14** (accession number 47QH) and compound **39** (accession number 4YS7) have been deposited in the Protein Data Bank, Research Collaboratory for Structural Bioinformatics, Rutgers University, New Brunswick, New Jersey.

* Corresponding author.
E-mail address: douglas.burdi@sunovion.com (D.F. Burdi).
† Present address: Epizyme Inc., 400 Technology Square, 4th Floor, Cambridge, MA 02139, United States.
‡ Shanghai ChemPartner, Ltd, 965 Halei Rd., Zhangjiang Hi-Tech Park, Pudong New Area, Shanghai 201203, China.
§ PharmAdvance, 159 Middle Chengjiang Rd., Hi-Tech Park, D501, Jiangyin, Jiangsu 214431, China.
¶ Present address: Fudan University, Zhangjiang Institute, Center for Drug Discovery & Development, 826 Zhangheng Rd., Pudong, Shanghai 201203, China.
|| Present address: Constellation Pharmaceuticals, 215 First Street, Suite 200, Cambridge, MA 02142, United States.

http://dx.doi.org/10.1016/j.bmcl.2015.03.050
0960-894X/

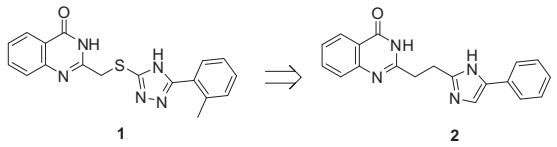

Figure 1. Evolution of the lead series.

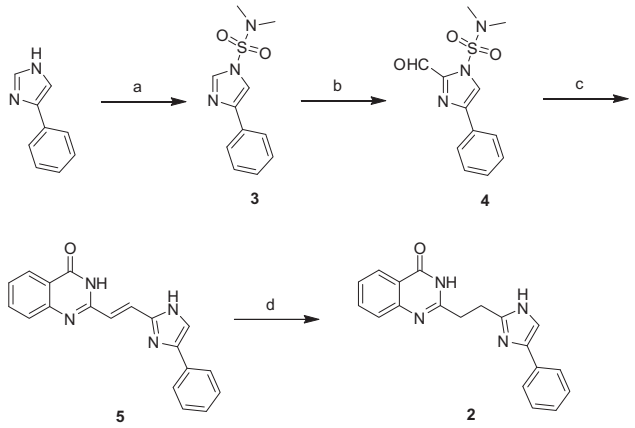

Scheme 1. Reagents: (a) dimethylsulfamoyl chloride, K_2CO_3, DMF; (b) LDA, DMF, THF; (c) 2-methylquinazolin-4(3*H*)-one, $ZnCl_2$, HOAc; (d) H_2, Pd/C, MeOH.

We began our SAR survey of this series by examining a series of azole isosteres, and we quickly realized that additional heterocycles beyond imidazole were not tolerated at this position (see Supplemental information).[9] We then turned our attention to the bicyclic ring on the left-hand side of the molecule.

Table 1 shows a representative set of SAR for a variety of bicyclic substituents on the left-hand side of our lead series. In order to gain a better understanding of how ADME correlates with other physicochemical properties, we also gathered data on human microsomal clearance. Several SAR trends are apparent. Carbocyclic and monocyclic rings, as in **9** and **12**, respectively, were not tolerated, but incremental improvements in the potency of the bicyclics were realized by the introduction of one nitrogen, as in **10** and **11**, and then two nitrogens, as seen in **13**–**16**. Compounds possessing the oxa-quinazoline ring, such as **2**, showed better microsomal stability than their quinazoline counterparts such as **13**. Heteroatom substituents on the oxa-quinazoline ring, as seen in **6** and **7**, were tolerated, but exocyclic substituents at these positions, as in **8**, were not. Finally, methylation of the imidazole ring at either nitrogen or carbon, as seen in **15** and **16**, respectively, led to some loss in potency, but N-methylation in particular led to improvements in in vitro microsomal intrinsic clearance. While we were pleased to see achievement of single-digit nanomolar potency with **14**, we were still troubled by its poor microsomal stability. The combination of good potency and microsomal stability, at this juncture, remained elusive (Table 2).

Based on metabolite ID studies which identified the aryl substituent of the imidazole as a probable site of metabolism, we turned our attention to aryl substitutions of the imidazole ring with the hope of attenuating in vitro intrinsic clearance. Table 2 shows a series of aryl- and heteroaryl-substituted imidazoles, where some trends in the SAR are readily apparent. N-methylation of the imidazole ring usually improved microsomal stability, as seen in the comparison between phenyl analogs **14** and **17** and furans **18** and **19**. Addition of a 3-fluoro substituent to the phenyl ring, as in **20**, resulted in a slight loss of potency relative to **14**, and failed to reduce in vitro microsomal clearance. Replacement of the

Table 1
Representative bicycles on the left-hand side of the phenyl-imidazole series

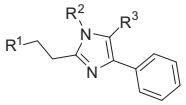

R^1	R^2	R^3	ID	IC_{50} (μM)	HLM (μL min^{-1} mg^{-1})
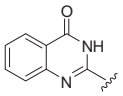	H	H	**2**	0.065	73.9
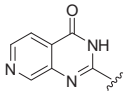	H	H	**6**	0.320	28.0
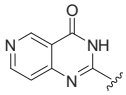	H	H	**7**	0.150	39.8
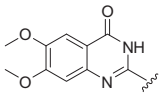	H	H	**8**	>10	nt
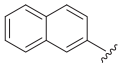	H	H	**9**	>10	226
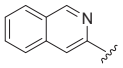	H	H	**10**	0.480	207
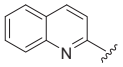	H	H	**11**	0.225	529
	H	H	**12**	>10	nt
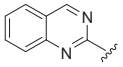	H	H	**13**	0.060	242
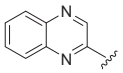	H	H	**14**	0.009	229
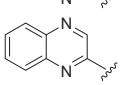	H	Me	**15**	0.110	178
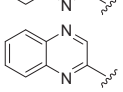	Me	H	**16**	0.090	55

phenyl substituent with a 4-pyridyl heterocycle, as in **21**, voided activity, while the 3-pyridyl substituent seen in **22** and **23** was tolerated. Although we were encouraged by the favorable microsomal stability of **23**, its potency was insufficient for lead advancement, so we began to explore other scaffold opportunities for improving affinity.

During the course of hit refinement, we had an opportunity to co-crystallize several of our actives with human PDE10A. Figure 2 shows a co-crystal structure of **14** with human PDE10A. The phenyl imidazole resides in the selectivity pocket[10] with the imidazole nitrogen forming a hydrogen bond with the side-chain hydroxyl group of Y693. Interestingly, the phenyl ring is nearly coplanar with the imidazole ring, and this observation would become important for our scaffold designs. The quinazoline ring resides deeper in the active site where it is sandwiched in the hydrophobic clamp defined by F696 and F729; the ring nitrogen forms a hydrogen bond with Q726.

The co-crystal structure proved useful in our efforts at structure-based drug design. Based on the aforementioned co-planarity of the phenyl and imidazole rings in the co-crystal structure of **14**, we reasoned, as shown in Figure 3, that fusion of the pyridine